Lateral Dispersion from Tall Stacks

STEVEN R. HANNA*

Environmental Research & Technology, Inc., Concord, MA 01742

(Manuscript received 9 November 1985, in final form 29 March 1986)

ABSTRACT

Hourly ground-level concentrations of SF_6 at downwind distances ranging from 0.5 to 50 km were observed by the Electric Power Research Institute (EPRI) on dense monitoring networks around power plants at Kincaid, Illinois, and Bull Run, Tennessee. Sigma y on given sampling arcs was estimated by a robust procedure. Over 160 h of data are available from monitoring arcs located at about five downwind distances, which show that σ_y is close to linear with downwind distance, x. During unstable conditions, $\sigma_y u/w_* x = 0.6$. When all the data are plotted together, the following empirical equation is valid:

$$\sigma_y u/\sigma_v x = \langle 1 + 0.9\{x/[(u)(15\,000\text{ s})]\}^{1/2}\rangle^{-1}.$$

1. Introduction

The purpose of this paper is to present the results of the analysis of an extensive new set of lateral dispersion observations. The data were taken by the Electric Power Research Institute (EPRI) at power plant sites in Kincaid, Illinois, and Bull Run, Tennessee. Formulas for σ_y are presented which provide good agreement with the field data.

Lateral dispersion of smoke plumes is far easier to observe than vertical dispersion because it can be determined from a network of monitors at the ground surface. For the past 50 years scientists have been using a variety of tracers and monitoring equipment to measure the standard deviation, σ_y, of the lateral concentration distribution. In some cases mobile monitors mounted in vehicles are used to observe lateral dispersion. Review papers by Gifford (1976) and Draxler (1984) provide excellent summaries of the experiments at downwind distances less than about 100 km. Observations of lateral dispersion at larger downwind distances (100 km or more) are reviewed by Gifford (1977, 1982). Experimental procedures are reviewed by Johnson (1983).

In all of these studies, σ_y is proportional to x at very short times or distances. But the data put us in somewhat of a dilemma because many of the short-range data suggest that σ_y is proportional to x raised to a power ranging from 0.5 to 0.9 at the most distant monitors ($10 < x < 100$ km). In contrast, the long range regional data reported by Gifford suggest that σ_y continues to be proportional to x at distances out to 1000 km or more. These differences may be due to the effects of averaging and sampling times, although no one has systematically studied all short-range and regional data with the purpose of explaining the discrepancies.

Differences in σ_y observed by different experimenters may be due to the mathematical procedures used to calculate σ_y. It is generally assumed that plumes have a Gaussian distribution, but experience has shown that the distribution during any given experiment may be highly non-Gaussian. For example, the plume may be skewed or may consist of two or more segments. Some experimenters calculate σ_y using the moment method and some use the best-fit-Gaussian method. The moment method is strongly influenced by outliers. Other difficulties arise when the ratio σ_y/x is larger than 0.5 if the data were taken along a straight line (in a Cartesian coordinate system), since the diffusion process is taking place in a polar coordinate system. For example, if the plume is uniformly distributed in all directions around the source then the σ_y calculated from data on a straight line is irrelevant. Fortunately, the EPRI monitors were placed on arcs rather than straight lines.

There are almost as many σ_y models or formulas as there are σ_y experiments. Irwin (1983), Gifford (1982), Draxler (1984) and Briggs (1985) discuss several of the proposed formulas, most of which can be written in the form

$$\sigma_y \approx \sigma_v t \phi(t/T_{Ly}) \tag{1}$$

where σ_v is the lateral turbulence velocity and T_{Ly} is the Lagrangian time scale in the lateral cross-wind direction. Several researchers have proposed that $\phi(t/T_{Ly}) = (1 + t/2T_{Ly})^{-1/2}$, which closely agrees with Taylor's (1921) theory. As Pasquill and Smith (1983) warn, one

* Present affiliation: Sigma Research Corporation, Lexington, MA 02173.

of the problems in interpreting Eq. (1) is that a certain sampling time, T_s, is implied. The early Pasquill (1961) σ_y curves were intended to apply to sampling times of 3 to 10 min. Thus, it should be no surprise that the Pasquill σ_y curve for stability class E (slightly stable) would underestimate σ_y data taken during a 1-h sampling period, since there is much more mesoscale lateral turbulent energy that is picked up by the 1-h plume (Hanna 1983). Pasquill and Smith (1983) suggest formulas for accounting for the effects of travel time, sampling time and averaging time, but the formulas generally require a knowledge of the energy spectrum and are not used in routine applications. In this paper the discussion is limited to a 1-h sampling time.

2. Selection of hours and preparation of data set

A comprehensive SF_6 tracer study was conducted during 1980 and 1981 around the Kincaid power plant in central Illinois. Bowne et al. (1983) provide an overview of the Kincaid study. An injection of SF_6 was made into a 183-m stack and hourly average ground level concentrations were observed by a network of about 200 monitors. The positions of the monitors were shifted each day based on the observed wind direction and the predicted downwind distance to maximum ground-level impact. Figure 1 provides an example of the monitor locations during one of the experiments at Kincaid. A similar measurement program took place in 1982 around the Bull Run, Tennessee, power plant, which has a 244-m stack (Bowne et al., 1984). The terrain is flat at Kincaid and is moderately complex (100-m ridges) at Bull Run.

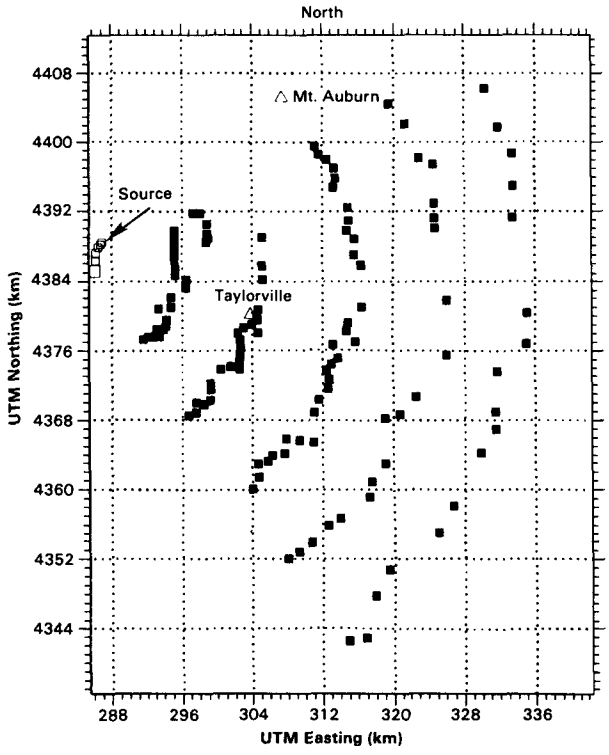

FIG. 1. Tracer sampling array of SF_6 at Kincaid for neutral conditions and westerly winds.

The overall purpose of our study is the development of an improved dispersion model for tall stacks. The data set was divided into hours to be used for developmental work and for final testing. The 90 h from Kincaid and 71 h from Bull Run that are analyzed here represent only about 50% of the total developmental data set. Many hours are not included because concentrations were very low, the plume was on the edge of the monitoring network, or the plume was very "spotty" (i.e., scattered spots of low to medium concentrations). During each hour the monitors were arbitrarily assigned to several arcs at fixed distances from the plant. Distances of 0.5, 1, 2, 3, 5, 7, 10, 15, 20, 30, 40 and 50 km were used, although on a given hour only five to seven of these arcs had monitors on them. In some cases at Bull Run the monitoring arcs extended completely around the stack. Even though a particular hour was selected for the σ_y analysis, not all of the arcs with data during that hour may have been used. Some arcs were filtered out because of low concentrations or because the plume was on the edge of the arc. A total of 493 σ_y estimates from Kincaid and 230 σ_y estimates from Bull Run were available for analysis.

Some of the lateral concentration distributions were non-Gaussian, with portions of plume material lying outside of the main body of the plume. The outliers can very strongly influence the σ_y estimate if one of the usual methods is used (i.e., the moment method or the best-fit-Gaussian curve method). Consequently, the "cumulative distribution" method, in which it is assumed that the arc distance from the y location of the 16th percentile to the y location of the 84th percentile of $\int C dy$ equals $2\sigma_y$ (see Fig. 2), was used in this analysis. The assumption is exactly correct for a Gaussian distribution. The procedure is robust in that it is not very sensitive to the influence of outliers on the σ_y estimate. We emphasize that our estimates of σ_y employ data along arcs rather than straight lines.

Besides the direct observations of σ_y at given distances x, several other parameters are needed for the analysis. The wind speed, u, and lateral turbulence velocity, σ_v, are observed at a height of 100 m on a meteorological tower. The mixing depth, h, is obtained from a boundary layer model prediction scheme similar to Carson's (1973) method. The convective velocity, w_*, is obtained from both the observed wind speed and a parameterization of the surface heat flux, which is based on incoming solar radiation and ground and vegetation conditions (Holtslag and Van Ulden, 1983).

Most of the experiments took place during the daytime. Since emissions are from tall stacks (183 m at Kincaid and 244 m at Bull Run) and buoyancy fluxes are usually large ($F \approx 1000$ m^4 s^{-3} at each site), the

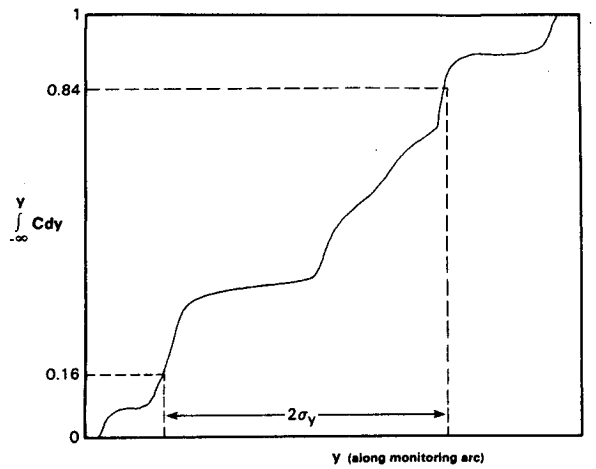

FIG. 2. Illustration of cumulative distribution method for estimating σ_y. With the EPRI data, the distance y is measured along an arc.

effective plume height is typically about 500 m and very little tracer material is diffused to the ground during stable conditions. Consequently, σ_y could not be estimated during the early morning and late evening periods. The data hours with σ_y estimates from Kincaid are typically slightly unstable to moderately unstable. Because wind speeds are very low at Bull Run (typically 1 to 3 m s^{-1}) the data from that site are often very unstable. The value of the convective velocity scale, w_*, is about 1.5 m s^{-1} at midday during clear summer periods at both sites, and midday mixing depths are about 1000 to 2000 m. Specific information on meteorological and source parameters for each of the 161 h are too voluminous to list here but are given in the project reports (e.g., Hanna et al., 1985).

3. Results

The 723 σ_y observations have been plotted several ways in order to better understand the physical processes and test a few theoretical formulas: σ_y vs x, a separate plot for each day containing all hours of that day; σ_y vs x, a separate plot for each stability class; $\sigma_y u/x$ vs x; $\sigma_y u/x$ vs x/u; $\sigma_y u/\sigma_v x$ vs x; $\sigma_y u/\sigma_v x$ vs x/u; $\sigma_y u/w_* x$ vs x; $\sigma_y u/w_* x$ vs xw_*/uh; $\sigma_y u/w_* x$ vs xw_*^3/F; σ_y/x vs xw_*^3/F. These results are summarized in the following sections.

a. σ_y versus x, all hours of each day

Typical plots of σ_y vs x for several hours in a day at the Kincaid site are given in Figs. 3 and 4. It is evident that σ_y is nearly linearly related to x for these data, which extend out to 50 km in Fig. 3 and 20 km in Fig. 4. At any given downwind distance, the range in σ_y over all hours is a factor of 2 in Fig. 3 and a factor of 3 in Fig. 4. A linear relation,

$$\sigma_y = axw_*/u, \tag{2}$$

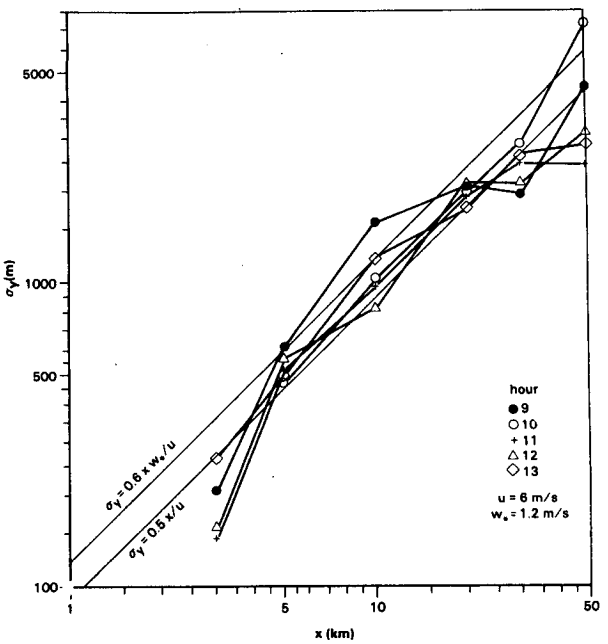

FIG. 3. σ_y vs x for 16 May 1981, SF_6 data at Kincaid. Conditions are slightly to moderately unstable.

with the constant a equal to about 0.4 to 0.6, provides a fair fit to the data on these figures and to the data from the other SF_6 experiments. This relation has been used by several other researchers studying dispersion in convective conditions. However, it is clear that another simple relation,

$$\sigma_y = 0.5\, x/u, \tag{3}$$

suggested by Heffter (1965), also fits these data fairly well. Equations (2) and (3) are further tested with the complete data set later.

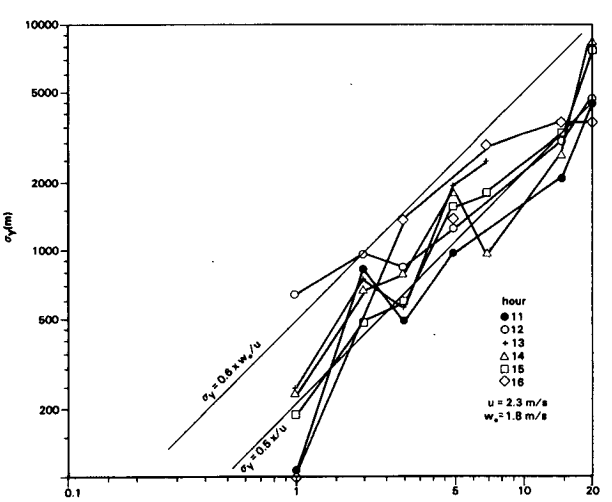

FIG. 4. σ_y vs x for 24 July 1980, SF_6 data at Kincaid. Conditions are very unstable.

b. σ_y versus x, by stability class

It is of interest to see how well the Kincaid σ_y data agree with the Pasquill–Gifford curves. Stability class was determined using the PPSP model preprocessor (Weil and Brower, 1984), which uses the ratio u/w_* to define ranges of stability classes in unstable conditions. All σ_y data from Kincaid for stability class 1 (very unstable) are shown in Fig. 5. Note that the downwind distance varies from 0.5 to 20 km for these experiments. The Pasquill–Gifford curve agrees with the data in the 1-km range, but underestimates the observed σ_y's by about 20% or 30% in the 10- to 20-km range. The linear relation,

$$\sigma_y = 0.24x \quad \text{(class 1)}, \tag{4}$$

passes near the median of the observations at each downwind distance. The trend of the data with downwind distance is seen to be slightly less than linear, with a best-fit power law exponent of about 0.9. On this figure 95% of the observations are within a factor of about 2 of the line given by Eq. (4).

The σ_y data from Kincaid for stability class 4 (neutral), plotted in Fig. 6, are chosen by the criterion $|L| > 100$ m (similar to the procedure suggested by Golder, 1972). The extrapolated Pasquill–Gifford curve is about a factor of 2 low at all distances. The linear relation,

$$\sigma_y = 0.12x \quad \text{(class 4)}, \tag{5}$$

slightly underestimates σ_y (by about 20%) at 1 km and slightly overestimates σ_y (by about 20%) at 50 km. Again, the trend of the data with distance is slightly less than linear, with a power law exponent of about 0.9. From similar graphs for classes 2 and 3, the following linear formulas are suggested:

$$\sigma_y = 0.20x \quad \text{(class 2)} \tag{6}$$

$$\sigma_y = 0.15x \quad \text{(class 3)}. \tag{7}$$

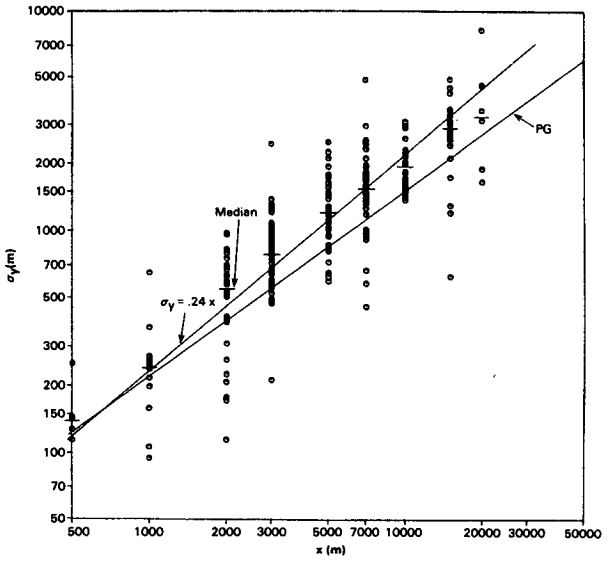

FIG. 5. σ_y at Kincaid as a function of downwind distance, x, for very unstable conditions (stability class 1). Curve for Pasquill–Gifford class 1 is drawn, as well as a best-fit linear curve. The median of the observed points at each downwind distance is indicated by a short horizontal line.

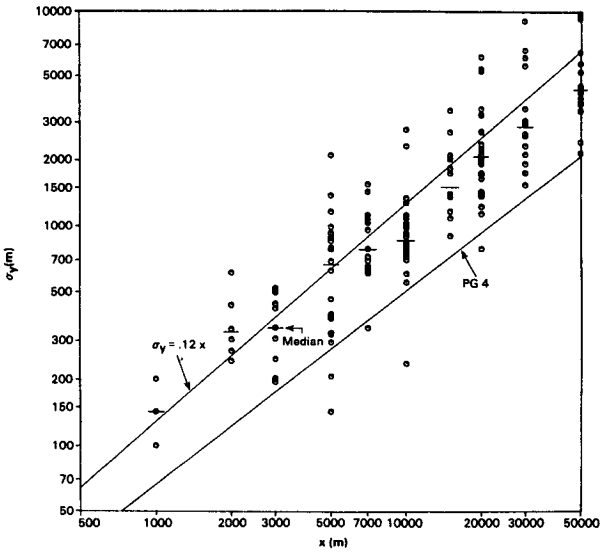

FIG. 6. σ_y at Kincaid as a function of downwind distance, x, for neutral conditions (stability class 4). The curve for Pasquill–Gifford class 4 is drawn, as well as a best-fit linear curve. The median of the observed points at each downwind distance is indicated by a short horizontal line.

c. $\sigma_y u/\sigma_v x$ versus x and x/u

The results of most theories suggest that the following relation is valid at small times for point sources with negligible buoyancy:

$$\sigma_y u/\sigma_v x = 1.0. \tag{8}$$

Gifford's (1982) data support the view that this linear law may be valid for travel times up to several hours. The turbulent velocity σ_v was observed at Kincaid at a height of 100 m, and has been used to produce Figs. 7 and 8. Very little dependence of $\sigma_y u/\sigma_v x$ with travel distance is evident for the Kincaid data in Fig. 7, which are best fit if the constant is changed to 0.75 in Eq. (8). On this figure, 95% of the data points are within a factor of 2 of this relation. The Bull Run data (not plotted here) also show very little dependence of $\sigma_y u/\sigma_v x$ on travel distance, and the best fit constant is about 1.2. Thus the average of the $\sigma_y u/\sigma_v x$ observations at Kincaid and Bull Run is about unity, in agreement with Eq. (8).

The relation suggested by Pasquill (1976) is also drawn on Fig. 7, showing that the slope of Pasquill's curve is clearly not in agreement with the data. In particular, Pasquill's curve is a factor of 5 below the observed median σ_y at a distance of 50 km.

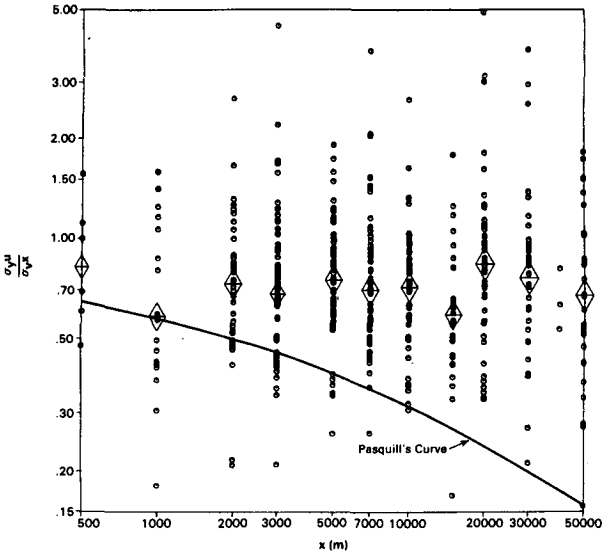

FIG. 7. The ratio $\sigma_y u/\sigma_v x$ as a function of x for Kincaid data. Pasquill's empirical curve is shown. The median of the observed points at each downwind distance is indicated by a diamond.

While Fig. 7 showed little variation of $\sigma_y u/\sigma_v x$ with travel distance, Fig. 8 shows that observations of this dimensionless combination at Kincaid do decrease slightly as travel time increases. Draxler (1976) suggested the following empirical formula, based on an analysis of data from several short-range dispersion experiments:

$$\frac{\sigma_y u}{\sigma_v x} = \frac{1}{1+0.9(x/uT_i)^{1/2}}. \tag{9}$$

He found that a value of 1000 s for the time scale, T_i, provided a best-fit to his elevated source data, but this value clearly leads to an underestimate of our σ_y data at large distances by a factor of 2 to 3. It is seen that a value of T_i equal to about 15 000 s better fits the data in Fig. 8.

A similar plot for the Bull Run data is given in Fig. 9, showing that the $\sigma_y u/\sigma_v x$ observations at Bull Run are about 50% greater than those at Kincaid. Equation (9) provides a fair fit to these data with T_i = 15 000 s and with the proportionality constant increased to 1.5. The vector wind speed is used for u in order to assure that the σ_v/u measurements are compatible with the σ_y measurements. Part of the discrepancy between the two power plant sites may be due to the strong influence of the plume buoyancy flux on σ_y at Bull Run, caused by the relatively low wind speeds at that site. The difference may also be caused by the fact that the 100 m wind and turbulence observations at Bull Run are taken from a tower mounted on a hill top, so that the observed σ_v/u may be representative of a height greater than 100 m above the average ground surface.

d. Analysis of $\sigma_y u/w_* x$ during convective conditions

During most sunny daytime periods, when the surface sensible heat flux is upward, the turbulent velocities are proportional to the convective velocity scale, w_*, which is defined by

$$w_* = (hg\overline{w'T'}/T)^{1/3} \tag{10}$$

where h is the mixing depth and g the acceleration of gravity. The proportionality constant between σ_v or σ_w

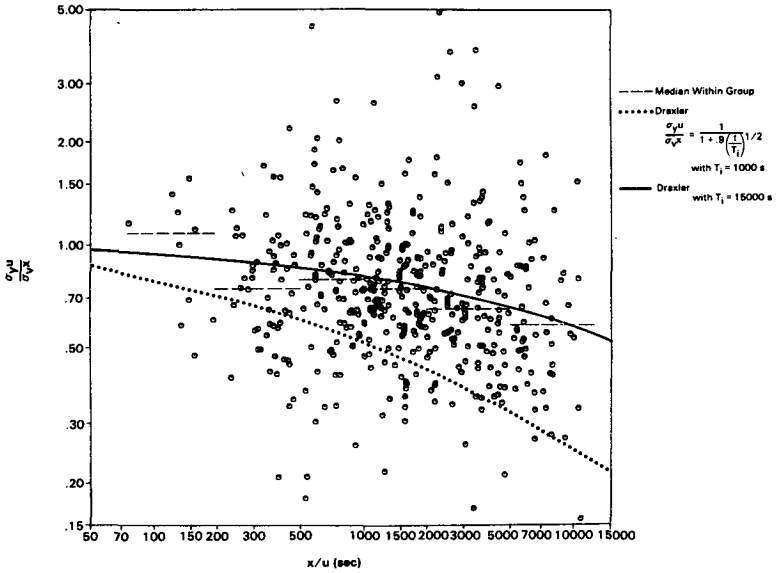

FIG. 8. The ratio $\sigma_y u/\sigma_v x$ as a function of travel time x/u for the Kincaid data. Two versions of Draxler's empirical formula are plotted, one using his suggested time constant, the other using a best-fit time constant.

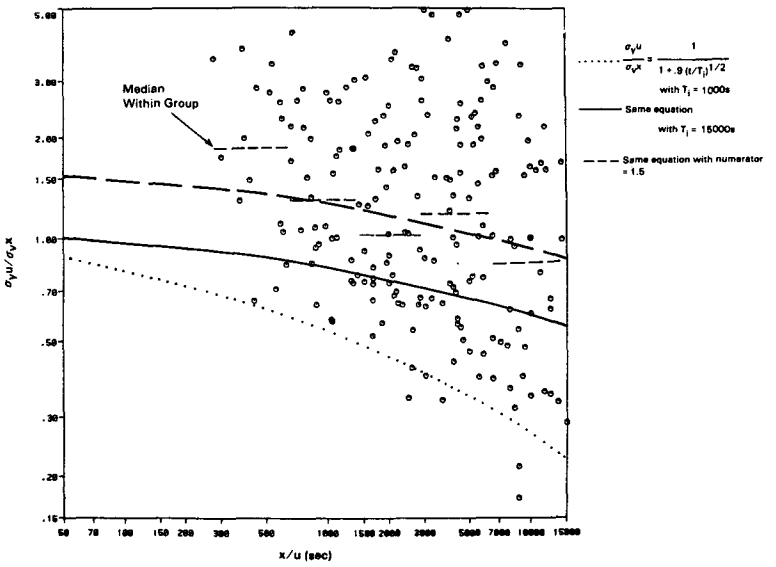

FIG. 9. The ratio $\sigma_y u/\sigma_v x$ as a function of travel time x/u for the Bull Run data. Three versions of Draxler's empirical formula are plotted, using different time scales and proportionality constants.

and w_* is found to be about 0.6. Consequently, Deardorff and Willis (1975) and others have proposed the following relation for nonbuoyant point sources:

$$\sigma_y u/w_* x = a\phi(X^*) \tag{11}$$

where a is a dimensionless constant and $\phi(X^*)$ is a dimensionless function of dimensionless distance $X^* = xw_*/uh$. Deardorff and Willis (1975) suggest

$$\left.\begin{aligned} a &= 0.51, \\ \phi(X^*) &= (1+0.91X^*)^{-1/2} \end{aligned}\right\}. \tag{12}$$

Lamb (1982) suggests $a = 0.33$ for plume centerlines of elevation greater than 0.1 h and $a = 0.60$ for plume centerlines of elevation less than 0.1 h. Briggs (1985) has the following suggestion:

$$\left.\begin{aligned} a &= 0.60, \\ \phi(X^*) &= (1+2X^*)^{-1/2} \end{aligned}\right\}. \tag{13}$$

Misra (1982) prefers $a = 0.4$. Thus the references yield estimates of a in Eq. (11) ranging from 0.33 to 0.60.

The Kincaid and Bull Run $\sigma_y u/w_* x$ observations are plotted as a function of X^* in Figs. 10 and 11. The data show little trend with increasing X^* and indicate a constant, a, of about 0.6. The slight upturn in $\sigma_y u/w_* x$ at small X^* for the Bull Run data may be due to plume buoyancy effects, which are discussed in section 3e. The Deardorff and Willis curve (Eqs. 11 and 12) and the Briggs (1985) curve underestimate the observed $\sigma_y u/w_* x$ on the figures by a factor of 2 or 3 at $X^* = 10$. Again, more than 95% of the points are within a factor of 2 of the simple formula:

$$\sigma_y u/w_* x = 0.6. \tag{14}$$

Data from other convective dispersion experiments are also plotted on Fig. 10. The Morgantown data are from van traverses of the plume from a power plant stack, the Cabauw data are from a monitoring network sampling the tracer plume from a neutrally buoyant release, and the BAO data are from lidar sampling of tracer material from a neutrally buoyant release. Briggs (1985) presents all these data in his Fig. 1. These other data are limited to X^* less than 4; i.e., the maximum dimensionless downwind distances are an order of magnitude less than those from the Kincaid and Bull Run data.

These other data tend to support the downward-sloping Deardorff and Willis or Briggs curves on the figure, rather than the notion that $\sigma_y u/w_* x$ equals a constant. The Kincaid and Bull Run data, on the other hand, show little if any decrease in $\sigma_y u/w_* x$ at large X^* (>1) and are far above the empirical curves at X^* ~ 20 or 30.

e. Plume buoyancy effects on σ_y

Both the Kincaid and Bull Run plumes are highly buoyant, with buoyancy parameter $F = (g/T_p)(T_p - T_a)w_s R^2$ equal to about 1000 m^4 s^{-3}. In this expression T_p is plume temperature, T_a air temperature, w_s plume vertical velocity and R stack radius. At small downwind distances for highly buoyant plumes, Briggs (1985) suggests the following formula for σ_y:

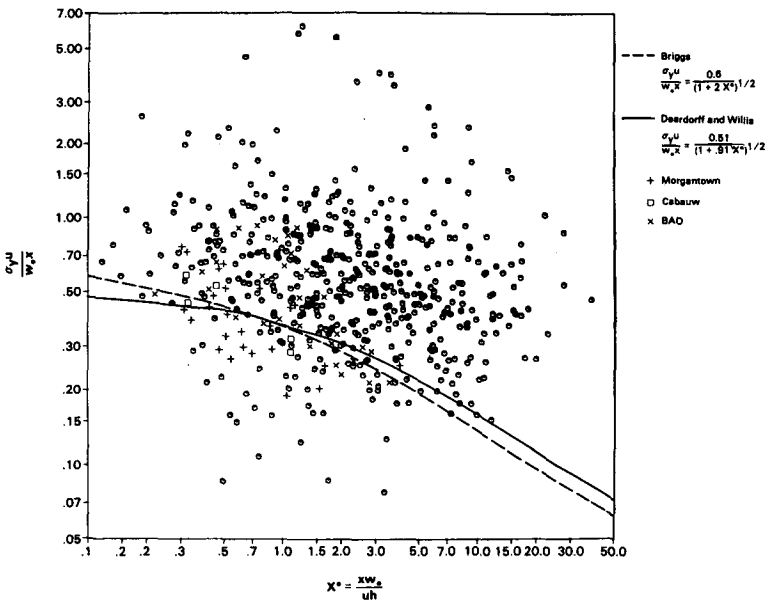

FIG. 10. Dimensionless sigma-y ($\sigma_y u/w_* x$) as a function of dimensionless downwind distance ($X^* = xw_*/uh$) at Kincaid. Data from other sites are plotted and two theoretical curves are drawn.

$$\sigma_y = 1.6F^{1/3}x^{2/3}. \quad (15)$$

Using convective scaling, this can be written

$$\sigma_y u/w_* x = 1.6F_*^{1/3}X^{*1/3} \quad (16)$$

where the dimensionless buoyancy flux F_* equals $F/w_*^2 uh$. Weil (1985) and Briggs (1985) recommend that Eq. (16) be used for small X^* and for F_* greater than 0.06. It can be shown that Eqs. (14) and (16) are equal when X^*/F_* equals 17. Thus a simple recommendation might be to use Eq. (16) for X^*/F_* less than 17 and Eq. (14) for X^*/F_* greater than 17.

As mentioned in section 3d, the underpredictions by Eq. (14) of the Bull Run σ_y data in Fig. 11 may be caused by the effects of plume buoyancy. The potential usefulness of Eq. (16), which accounts for plume buoyancy, is tested in Fig. 12 using data from Bull Run. The data do show a downslope with X^*/F_*, and the power law in Eq. (16) passes roughly through the middle of the data. However, the scatter is not significantly reduced from that in Figs. (10) and (11). It is important to note that the line from Eq. (16) does agree well with the data at low values of X^*/F_*, where the largest discrepancy between the two formulas would occur. The prediction from Eq. (16) for a typical value of F_* at Bull Run ($F_* = 0.2$) is sketched on Fig. 11, showing agreement with the median of $\sigma_y u/w_* x$ observations at small X^*.

4. Summary of formulas

The selected EPRI Kincaid and Bull Run σ_y observations are used to test various empirical and theoretical relations. The Pasquill–Gifford curves underestimate the observations at downwind distances out to 50 km, with a factor of 2 error for class D. The data also indicate that a linear relation between σ_y and x is valid out to distances of 50 km. Conversely, the drop-off of σ_y to a $\sigma_y \propto (x/u)^{1/2}$ relation that has been suggested by several references is not verified by these data.

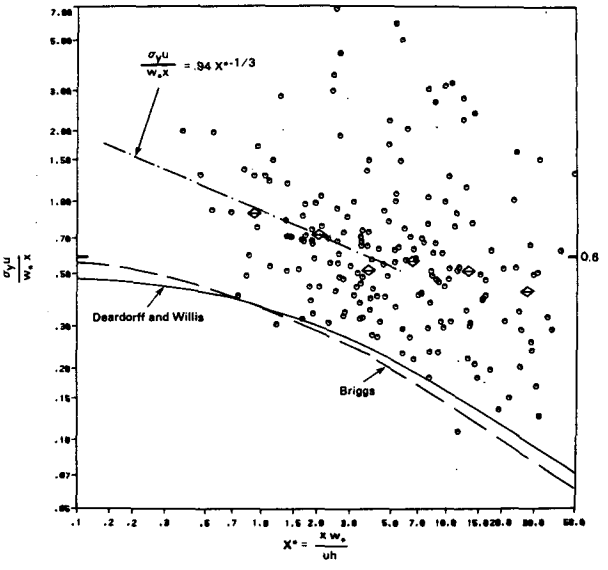

FIG. 11. Dimensionless sigma-y ($\sigma_y u/w_* x$) as a function of dimensionless downwind distance ($X^* = xw_*/uh$) at Bull Run. Diamonds are medians of points in groups. Solid and dashed lines are theoretical curves described in Fig. 10. Dash-dot line is theoretical curve from Eq. (16) for $F_* = 0.2$.

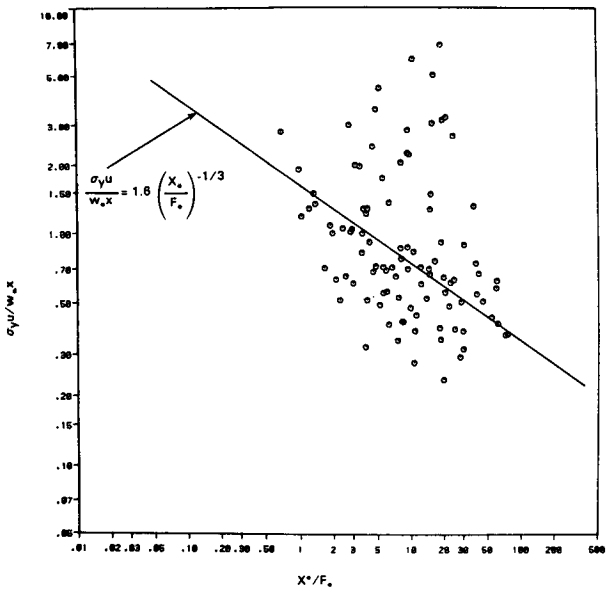

FIG. 12. Dimensionless $\sigma_y u/w_* x$ as a function of X^*/F_* at Bull Run. Equation (16) is plotted.

The following empirical formulas are valid:

$$\sigma_y u/\sigma_v x = 1.0/[1+0.9(x/uT_i)^{1/2}] \text{ with } T_i = 15\,000 \text{ s}$$

$$\sigma_y u/w_* x = 1.6(F_*/X^*)^{1/3} = 1.6(F/w_*^3 x)^{1/3} \quad \text{for} \quad X^*/F_* < 17$$

$$\sigma_y u/w_* x = 0.6 \quad \text{for} \quad X^*/F_* > 17$$

$$\sigma_y = 0.24x \quad \text{(class A or 1)}$$

$$\sigma_y = 0.20x \quad \text{(class B or 2)}$$

$$\sigma_y = 0.15x \quad \text{(class C or 3)}$$

$$\sigma_y = 0.12x \quad \text{(class D or 4).}$$

The reader is cautioned that false correlations may appear in a figure where a parameter such as the wind speed is used as part of the variables plotted on *both* axes. For example, the travel time on the abscissa in Fig. 8 is not observed directly but is calculated from x/u. But the wind speed is also used in the variable, $\sigma_y u/\sigma_v x$, plotted as the ordinate. Random variation in u will lead to an apparent decrease of $\sigma_y u/\sigma_v x$ with x/u, even if $\sigma_y u/\sigma_v x$ does not vary with x. Consequently, the agreement with Draxler's curve with T_i = 15 000 s may be accidental. This may also be true of the $\sigma_y u/w_* x$ versus xw_*/uh plot. The false correlation phenomenon is discussed in detail by Hicks (1978). It is not a problem in figures where the parameters that are plotted are independent (such as Figs. 3 through 6 in this paper).

Acknowledgments. This research was supported by the Electric Power Research Institute, with Dr. Glenn Hilst as Project Monitor. Many of the calculations and figures were made by Robert Paine of ERT. The author appreciates suggestions made by Dr. Jeffrey Weil of Martin Marietta Corporation.

REFERENCES

Bowne, N. E., R. J. Londergan, D. R. Murray and H. S. Borenstein, 1983: Overview, results, and conclusions for the EPRI Plume Model Validation Project: Plains site. EPRI Rep. EA-3074.

——, —— and ——, 1984: Summary of results and conclusions for the EPRI Plume Model Validation Project: Moderately complex site. EPRI Rep.

Briggs, G. A., 1985: Analytical parameterizations of diffusion: The CBL. *J. Climate Appl. Meteor.*, **24,** 1167–1186.

Carson, D. J., 1973: The development of a dry inversion-capped convectively unstable boundary layer. *Quart. J. Roy. Meteor. Soc.*, **99,** 450–467.

Deardorff, J. W., and G. E. Willis, 1975: A parameterization of diffusion into the mixed layer. *J. Appl. Meteor.*, **14,** 1451–1458.

Draxler, R. R., 1976: Determination of atmospheric diffusion parameters. *Atmos. Environ.*, **10,** 99–105.

——, 1984: Diffusion and Transport Experiments. *Atmospheric Science and Power Production,* D. Randerson, Ed., DOE/TIC-27601 (DE84005177), NTIS, 367–422.

Gifford, F. A., 1976: Turbulent diffusion typing schemes—A review. *Nucl. Saf.*, **17,** 68–86.

——, 1977: Tropospheric relative diffusion observations. *J. Appl. Meteor.*, **16,** 311–313.

——, 1982: Horizontal diffusion in the atmosphere: A lagrangian-dynamical theory. *Atmos. Environ.*, **16,** 505–512.

Golder, D., 1972: Relations among stability parameters in the surface layer. *Bound.-Layer Meteor.*, **3,** 47–58.

Hanna, S. R., 1983: Lateral turbulence intensity and plume meandering during stable conditions. *J. Climate Appl. Meteor.*, **22,** 1424–1430.

——, J. C. Weil, R. J. Paine, C. Burkhart and B. A. Egan, 1985: Plume model development and evaluation: Hybrid approach annual progress report. EPRI.

Heffter, J. L., 1965: The variation of horizontal diffusion parameters with time for travel periods of one hour or longer. *J. Appl. Meteor.*, **4,** 153–158.

Hicks, B. B., 1978: Some limitations of dimensional analysis and power laws. *Bound.-Layer Meteor.*, **14,** 507–509.

Holtslag, A. A. M., and A. P. Van Ulden, 1983: A simple scheme for daytime estimates of the surface fluxes from routine weather data. *J. Climate Appl. Meteor.*, **22,** 517–529.

Irwin, J. S., 1983: Estimating plume dispersion—A comparison of several sigma schemes. *J. Climate Appl. Meteor.*, **22,** 92–114.

Johnson, W. B., 1983: Meteorological tracer techniques for parameterizing atmospheric dispersion. *J. Climate Appl. Meteor.*, **22,** 931–946.

Lamb, R. G., 1982: Diffusion in the convective boundary layer. *Atmospheric Turbulence and Air Pollution,* F. T. M. Neiuwstadt and H. VanDop, Eds., Reidel, 159–230.

Misra, P. K., 1982: Dispersion of non-buoyant particles inside a convective boundary layer. *Atmos. Environ.*, **16,** 239–243.

Pasquill, F., 1961: The estimation of the dispersion of windblown material. *Meteor. Mag.*, **90,** 33–49.

——, 1976: Atmospheric dispersion parameters in Gaussian plume modeling. Part II: Possible requirements for change in the Turner workbook values. USEPA Rep., EPA-600/4-76-0306.

——, and F. B. Smith, 1983: *Atmospheric Diffusion.* 3rd ed., Ellis-Horwood, 437 pp.

Taylor, G. I., 1921: Diffusion by continuous movements. *Proc. London Math. Soc.*, **20,** 196.

Weil, J., 1985: Updating applied diffusion models. *J. Climate Appl. Meteor.*, **24,** 1111–1130.

——, and R. P. Brower, 1984: An updated Gaussian plume model for tall stacks. *J. Air Poll. Control Assoc.*, **34,** 818–827.